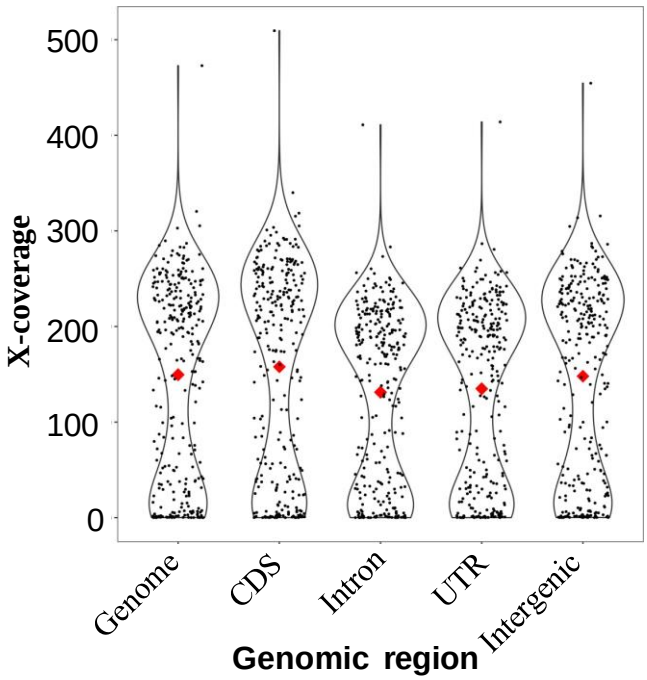

Figure S1: X-coverage profile of genomes sequenced. Samples with at least 10X coverage were considered for downstream analysis.

(a)

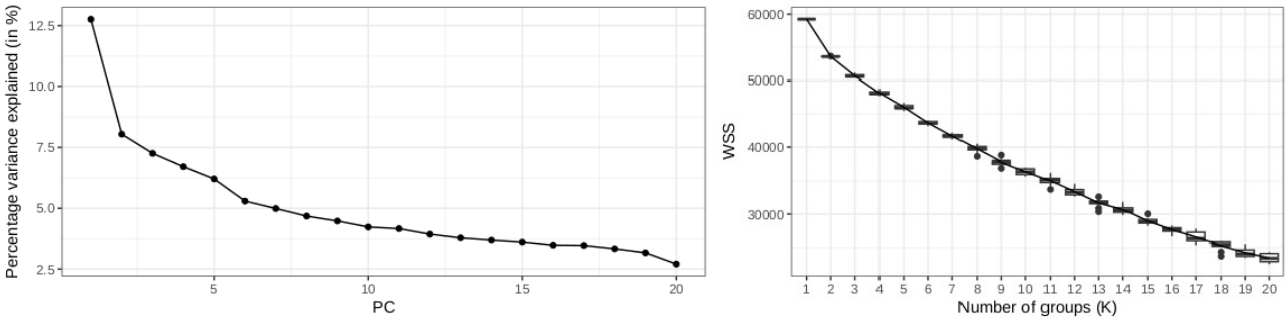

(b)

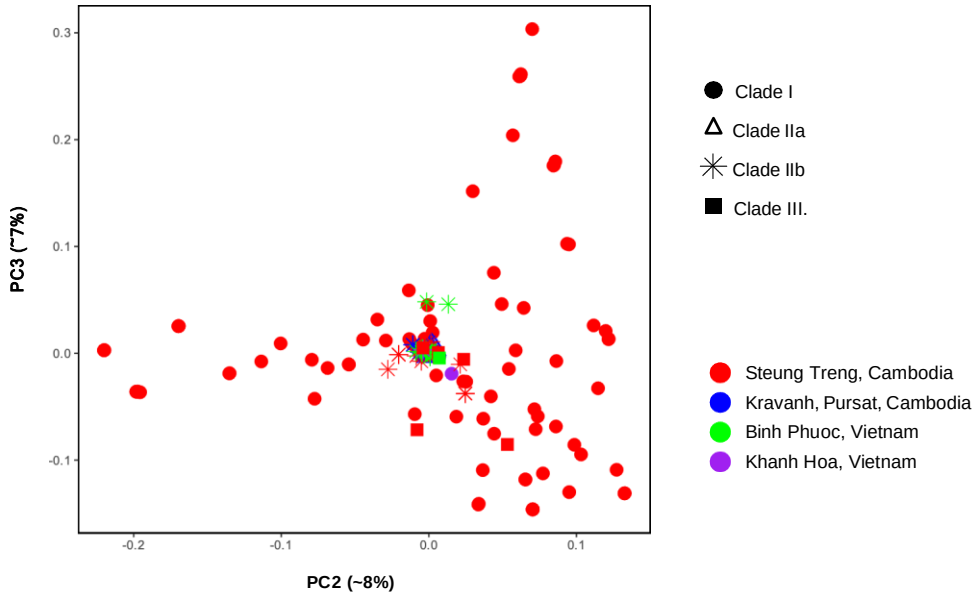

Figure S2: K-means clustering and PCA analysis: (a) PCA- based analysis to find the number of clusters from the SNP genotype. In this plot, the X-axis and Y-axis represent the principal components and the corresponding variance explained by the components. The highest drop in variance value was found from PC1 to PC2, after which the plot plateaued (on the left). K-means clustering analysis showed similar observations as the highest drop in With-in- Sum-of-Squares (WSS) was viewed between K1 and K2 indicating K=2 as the elbow point. (on the right) **(b)** Principal components 2 and 3 describe the variability within East Cambodian samples. The pattern of clustering supports the distinguished clades from phylogenetic analysis.

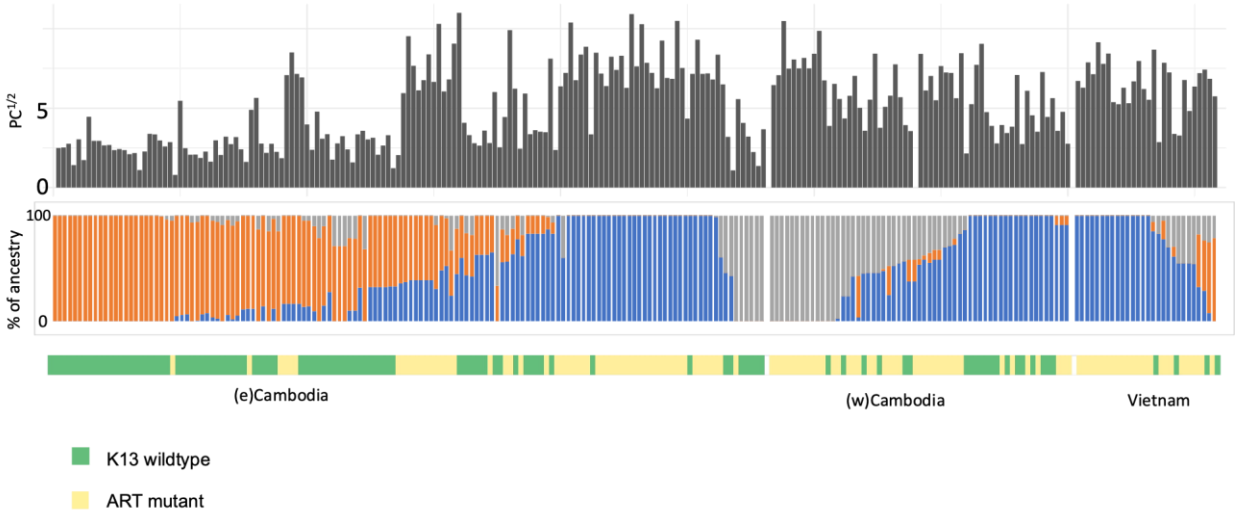

Figure S3: Admixture population analysis of parasite population. The bar graph (in the middle) shows the mixture of ancestries within parasites collected from three collection sites. The bar graph (on the top) shows the estimated parasite clearance half-life of each individual isolate. The heatmap at the bottom shows the K13 genotype. Strikingly a group of parasites from east Cambodia (left side of the plots) with a higher proportion of ancestral components shown by orange bar was found mostly to have $PC^{1/2}$ < 5 hours (susceptible parasites).

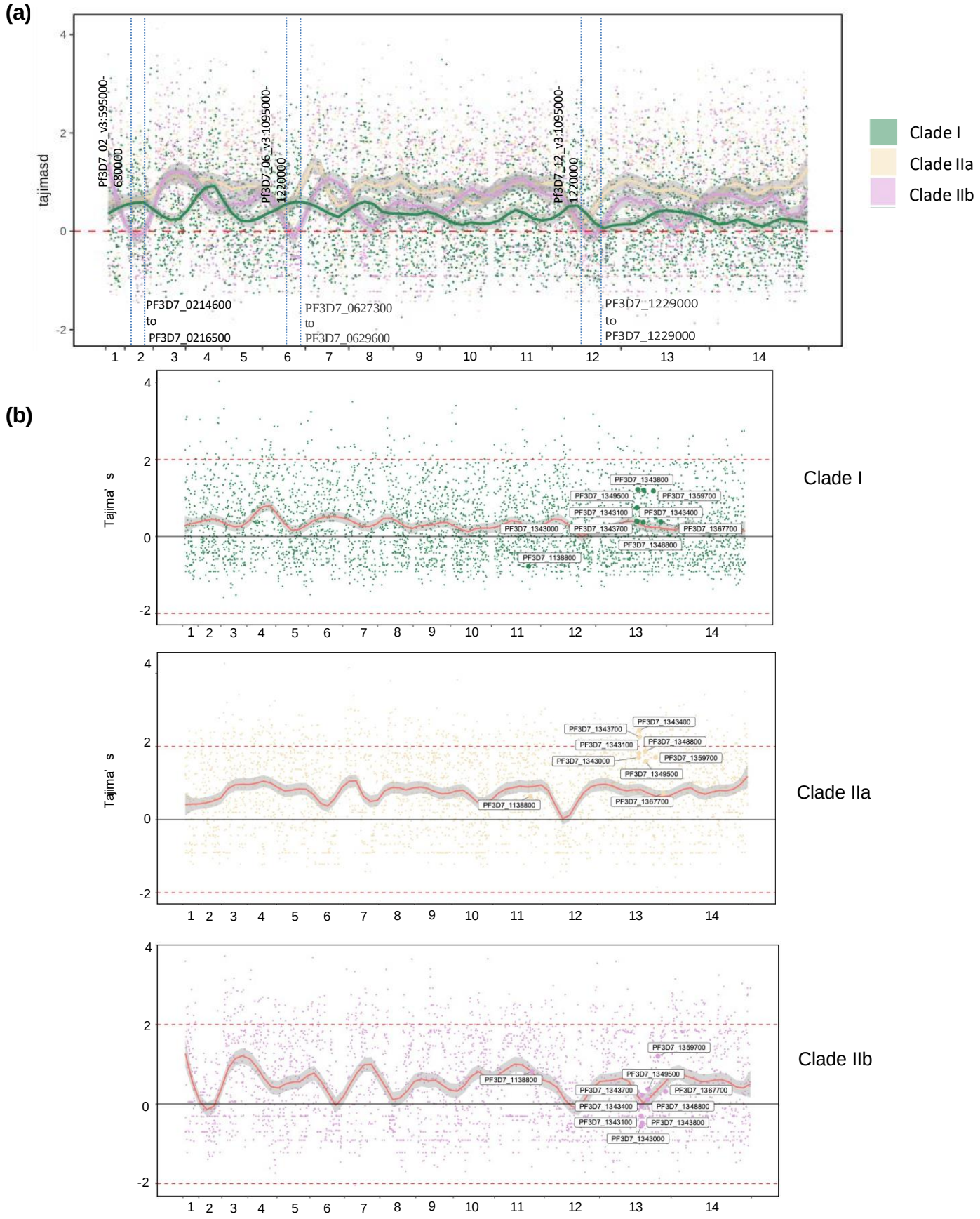

Figure S4: Genome-wide Tajima's D profile: (a) Value of Tajima's D for a non-overlapping 5 Kb window was applied to show difference selection pressure across the genome and for three different clades. It shows active selection pressure in at least three genome locations in subclade IIb and higher balancing selection in subclade IIa compared to clade I. (b) Gene-specific Tajima's D values were calculated and plotted for three individual clades. Phenotype-associated genes were labeled for individual clades. The corresponding table added as a supplementary table (Supp table 3).

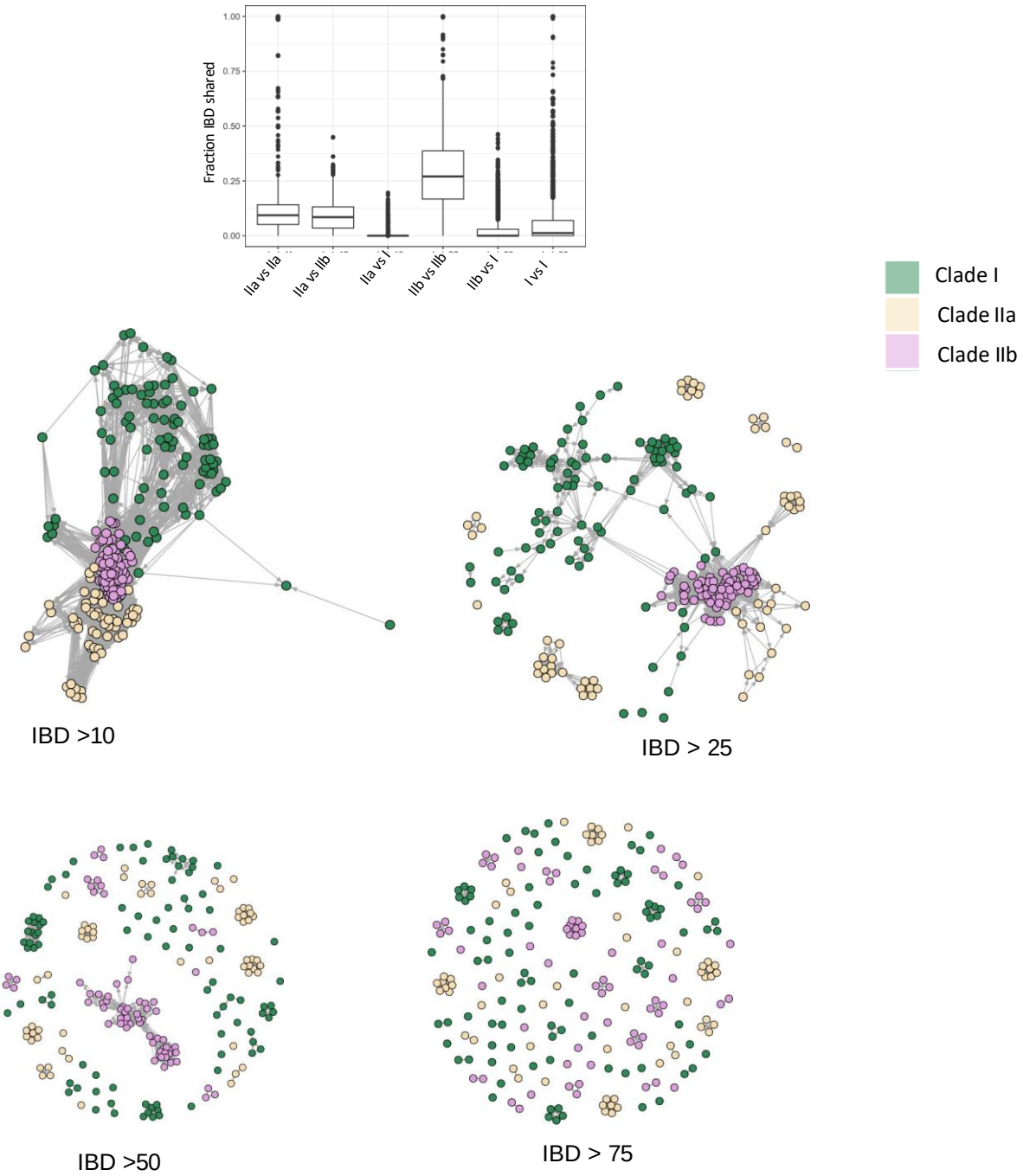

Figure S5: IBD analysis between clades. The box plot on top shows the lowest IBD sharing between clade I with clade IIa and clade IIb indicating the major genetic differences between these two groups supporting our ancestral and admixture group. Further IBD network shows relationships at different labels. It was clear that at IBD >25 clade IIb still remains well connected which further dissolves with higher sharing value. Lastly, there is no direct connection between clade I with clade IIa at even IBD > 10, indicating clade IIb as an admixture population and either of I or IIa as a founder/ancestral population.

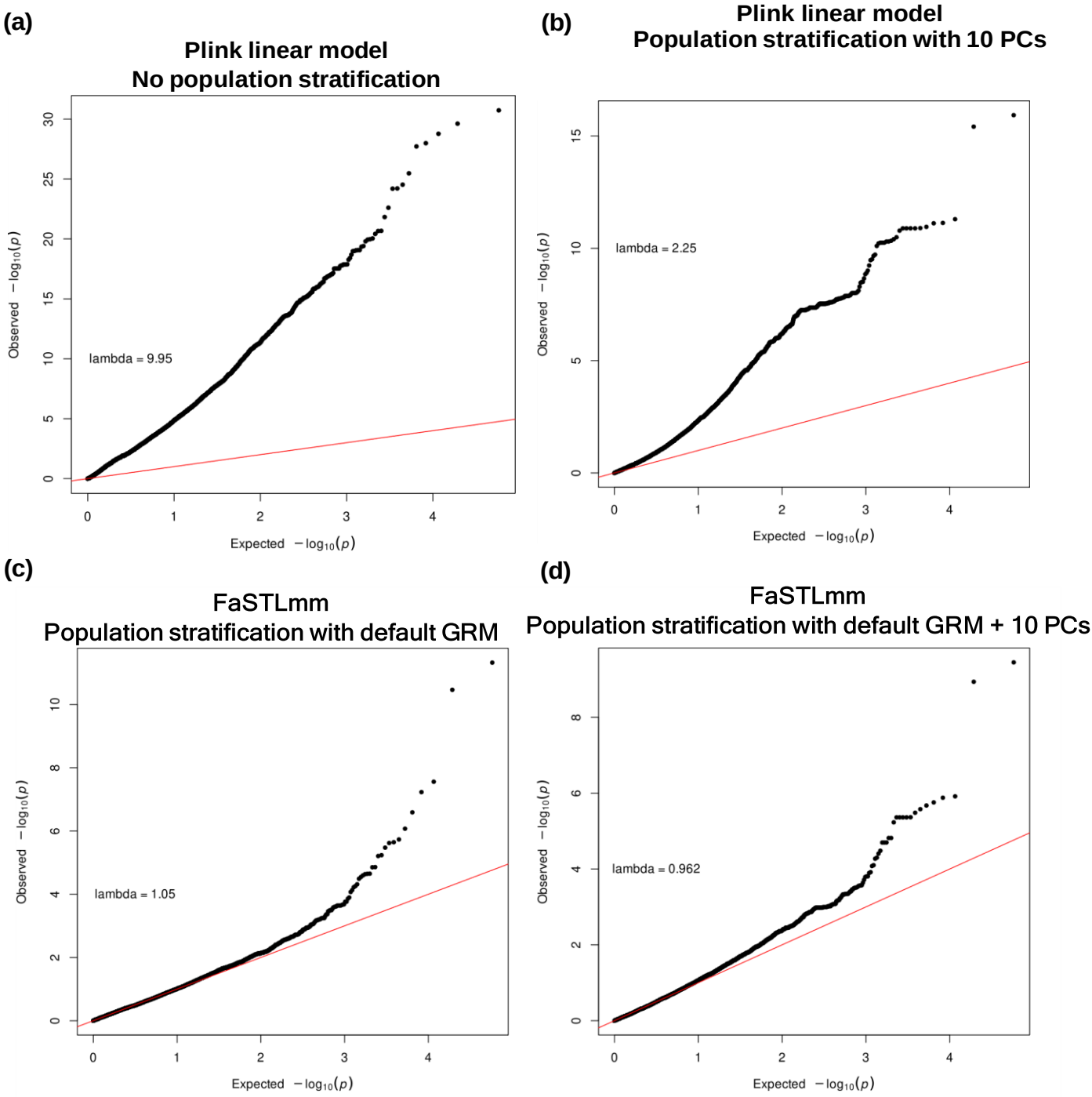

Figure S6: GWAS QQ plot with different configurations. (a-b) Plink association with linear model lambda being inflated as high as 9.95 (for no control of population structure) and 2.25 when 10 PCs were used for population stratification. (c) GWAS was performed with FaSTLmm Genetic Relatedness Matrix was used to control the effect of population structure (inflation rate as 1.05). (d). The genome-wide p-values were found deflated when GRM along with 10PCs were used as a control for population structure. Deflation was probably due to the implementation of population stratification by two mode s : GRM as well as PCs (being first two PC describe the population structure). Overall FaSTLmm showed the lowest acceptable range of lambda when GRM was used and was regarded as the result of association study.

(a)

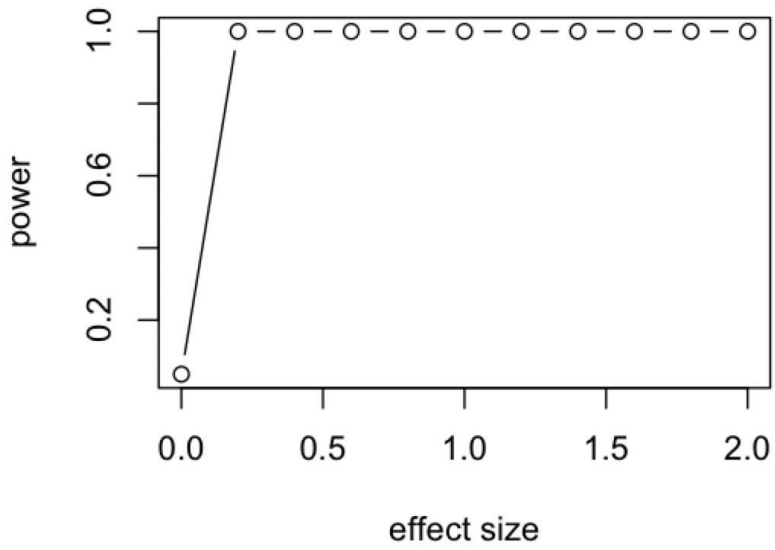

(b)

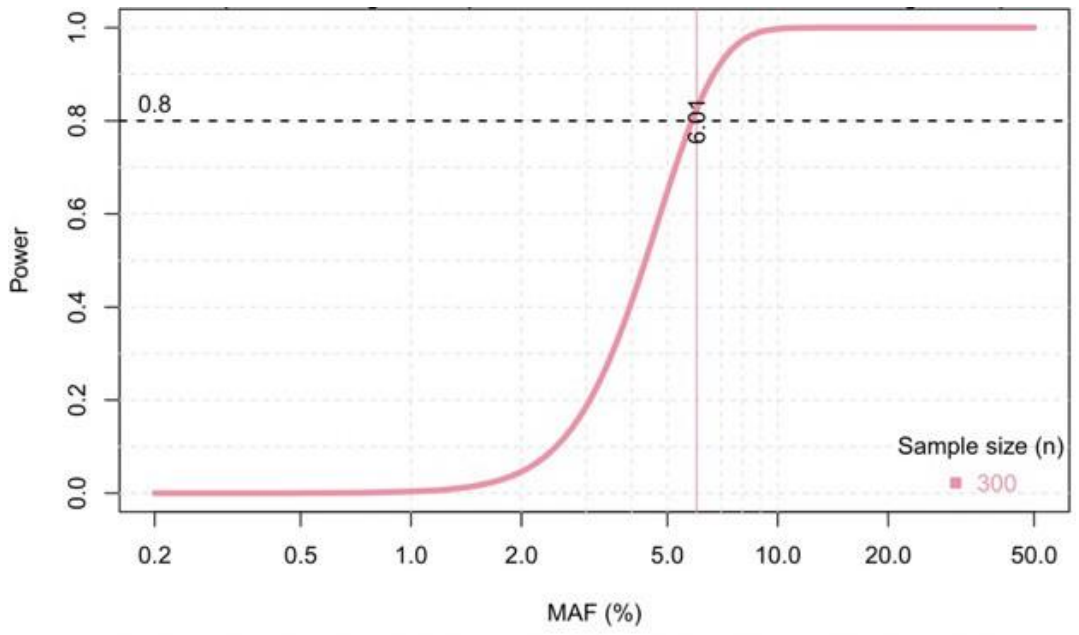

Figure S7: Power analysis of GWAS study (a) We have used the R package 'pwr' to find the optimum effect size to detect 80% power from the GWAS value for a degree of freedom = 1 and number of samples =300. We found that to achieve 80% power for detecting any association effect size of the SNPs should be around ~ 0.22. (b) Further powerEQTL package allowed us to estimate the minimum allele frequency required to achieve 80% power from association studies (since our phenotype is a continuous variable). The minimum MAF threshold needed to be 6.01 to achieve 80% power for detecting any association.

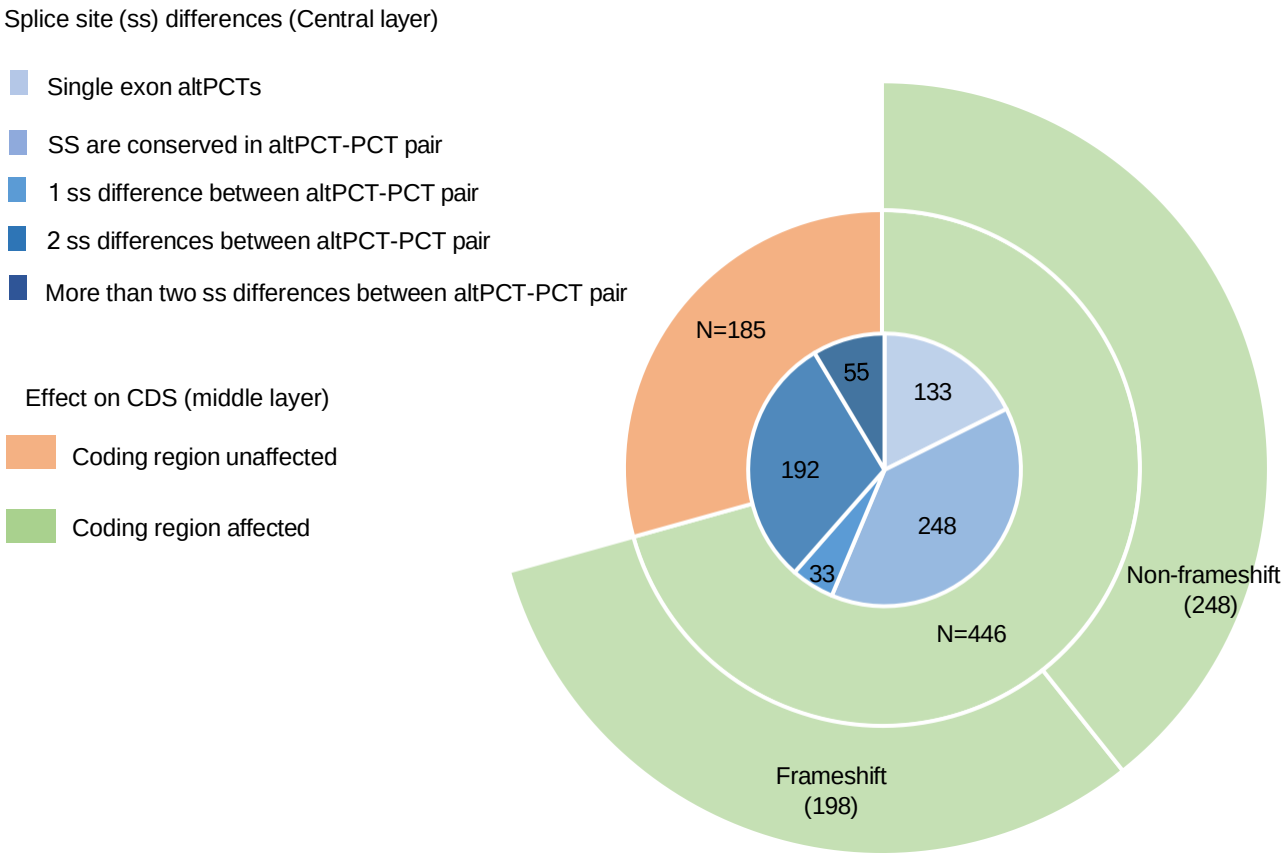

Figure S8: Classification of detected alternatively spliced PCTs. Comparing detected alternatively spliced PCTs with overlapping PCTs. (Central layer) First PCT-altPCT pairs were compared by differences in splice sites. (Middle layer) The second classification was based on coding region differences between the PCT-altPCT pair. (Outer layer) altPCTs with coding region differences further investigated whether to have a frameshift or non-frameshift effect. Data from the central layer are independent of the middle and outer layers.

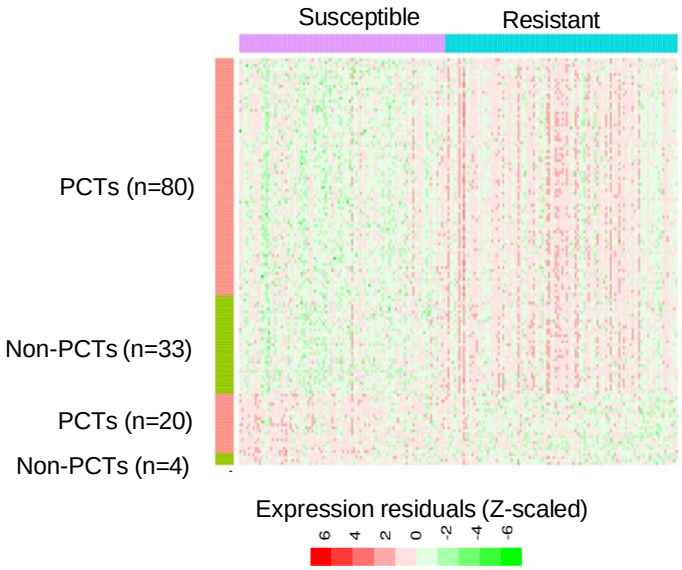

Figure S9: Differentially expressed transcripts from hr0 transcriptomes. Heatmap of differentially expressed transcripts between susceptible and resistant parasites with FDR <0.05 totaling 100 PCTs and 37 non-PCTs.

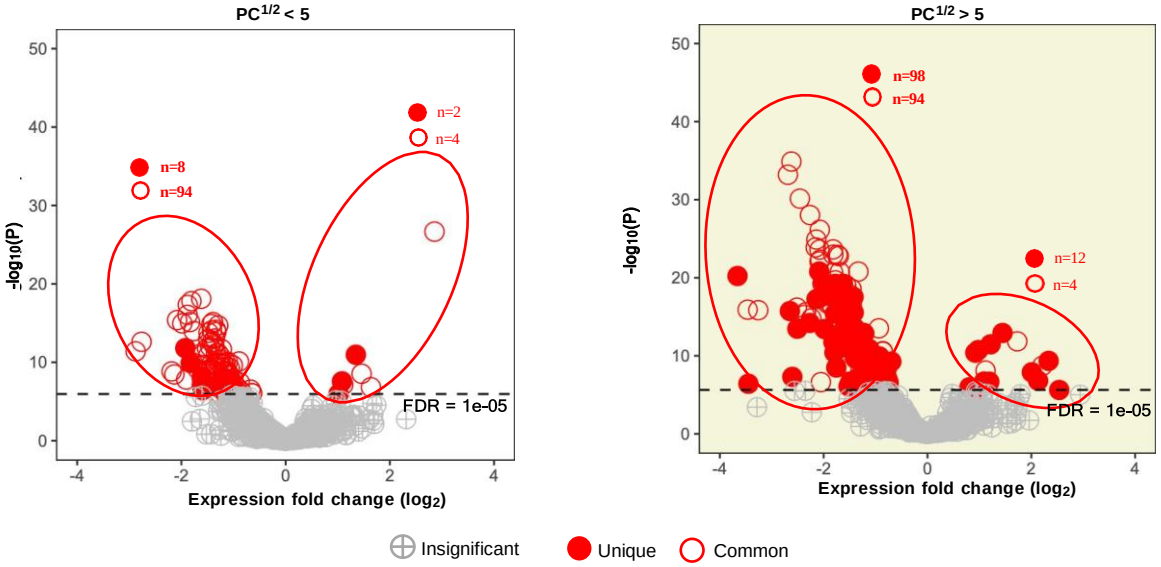

Figure S10: In-vivo transcriptome response to drug through non-PCRTs. Induction or repression of non-PCRTs upon treatment with artemisinin combination therapy in susceptible (left) and resistant (right) parasite groups. Any transcripts with FDR < 1e-05 considered as significant and commonly induced/repressed transcripts are marked as un-filled red colored circles. The background and point color of the volcano plots is to differentiate the resistant parasites from susceptible parasites and PCRTs from non-PCRTs respectively. White and beige background signifies the parasite groups as Susceptible and resistant respectively, whereas red circles here represent significantly up-down-regulated non-PCRTs.

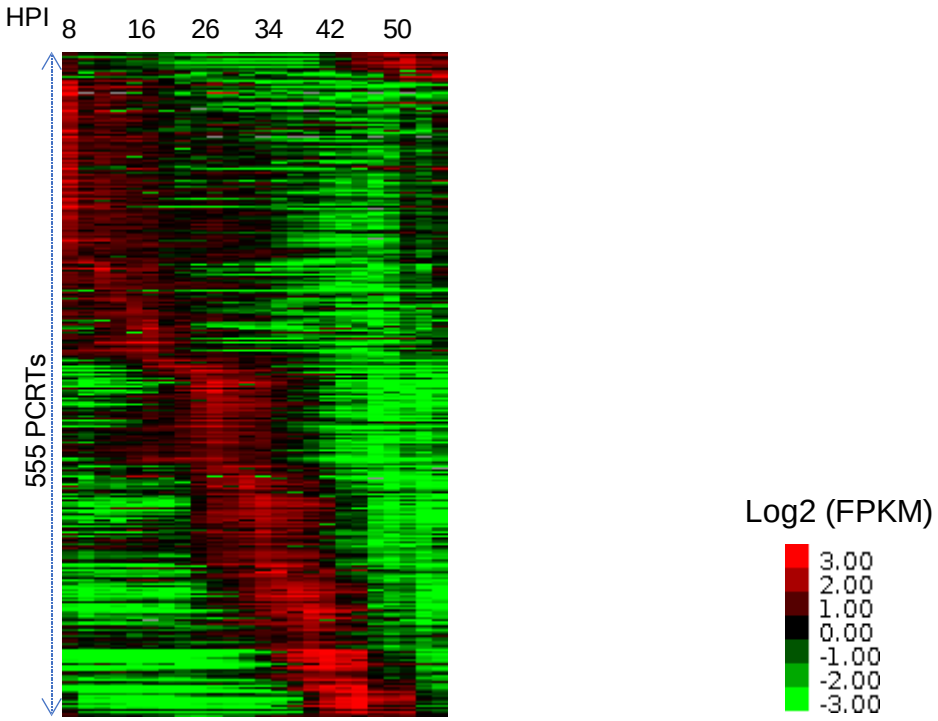

Figure S11: In-vivo repressed PCTs from IDC. Expression profiles of the PCRTs from intra-erythrocytic development cycle (IDC) repressed in resistant parasites upon 6 hours of exposure to ACT/TACT.

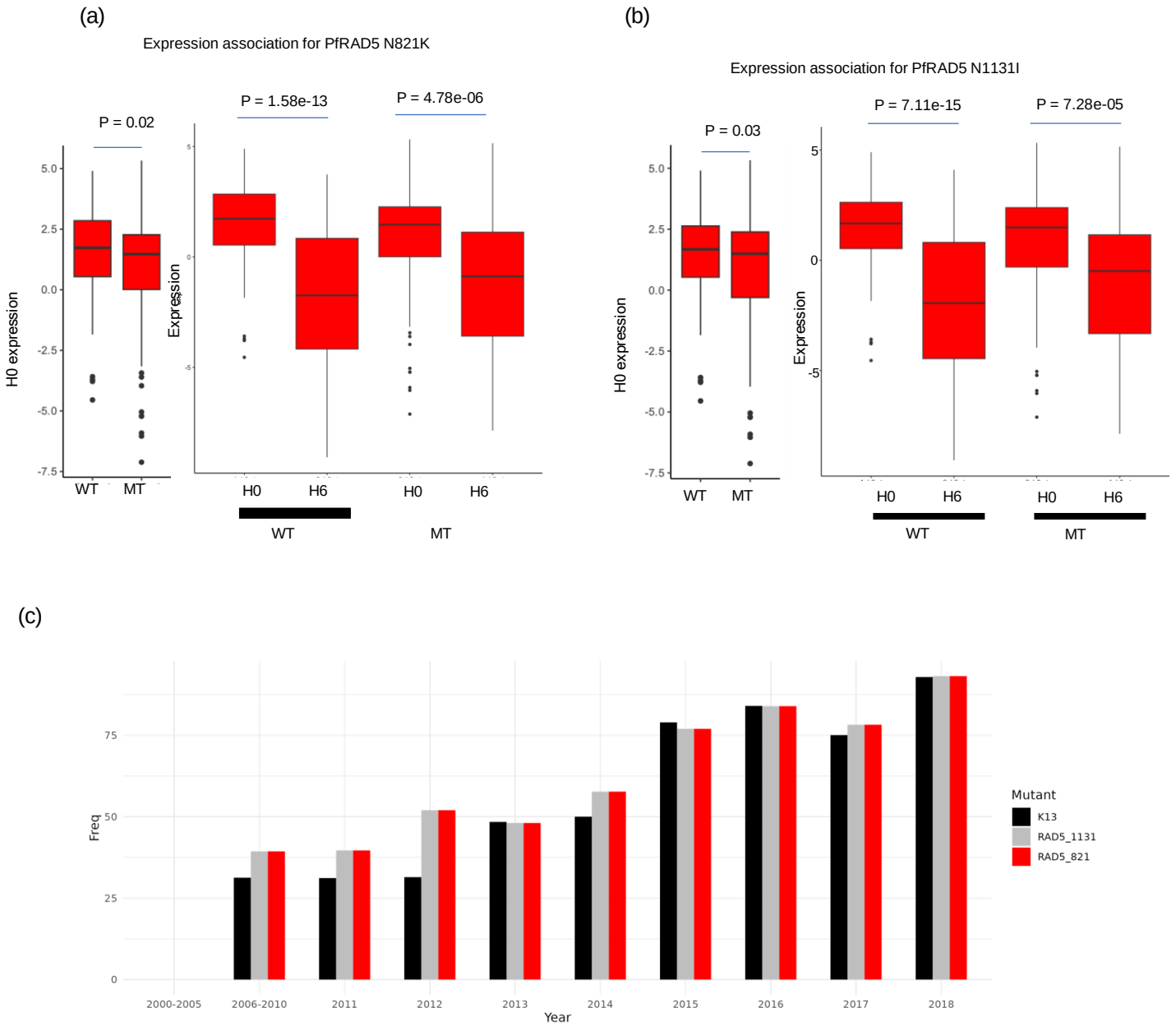

Figure S12: PfRAD5 mutations and altPfRAD5 expression. GWAS analysis detected two PfRAD5 mutations (N821K and N1131I) associated with parasite clearance half-life ($PC^{1/2}$). (a) An eQTL-like association was found for PfRAD5 N821K with expression of alternatively spliced PfRAD5 transcripts (left panel). Moreover, the expression of altPfRAD5 was repressed upon drug exposure in both resistant and susceptible parasites with a lower level of statistical significance for resistance parasites (right panel). (b) The second mutation, PfRAD5 N1131I, was found to be associated in an exactly similar way as PfRAD5 N821K. (c) Temporal change of frequencies for the two non-synonymous SNPs PfRAD5 N1131I and PfRAD5 N821K are highly correlated with PfK13 C580Y mutation from three countries (Cambodia, Thailand, and Vietnam) from eGMS from 2000 to 2018 (Pf7K data).

(a)

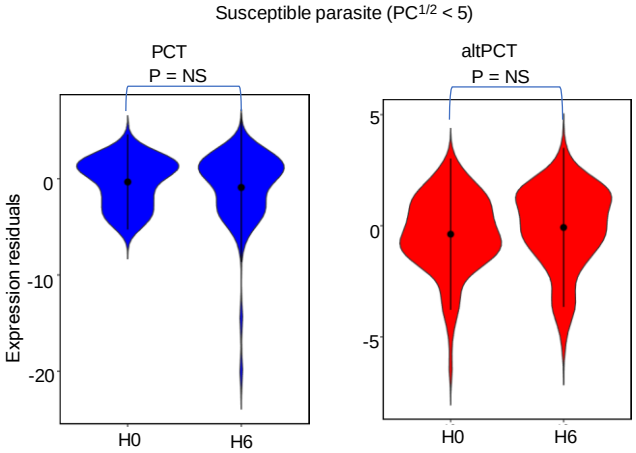

(b)

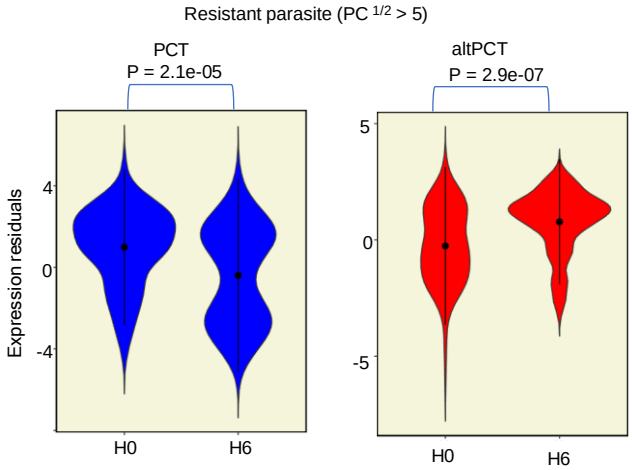

Figure S13: PfWD11 as a novel marker for artemisinin resistance. (a) From the in-vivo response study, no significant changes in the expression level were noticed for susceptible parasites for both PCT and altPCT of PfWD11. (b) PCT of PfWD11 was found down-regulated and altPCT up-regulated in response to drug exposure in resistant parasites.

(a)

Target	Forward primer	Reverse primer
Both isoforms	TGACCTTATGAACATTGATGAAAG	TCCATGGTACTTTTAATTTCTTGTG
Alternative isoform (altPCRT)	ATTTATTGGTTACTGCTTCTTGT	CCATGTTTATATTTTATTTAATTTTTTTCCCAACC
Canonical isoform (PCRT)	TATAATTGTTCAAAAGCATCACAAGAAA	TGGAATAGTGCACACCAAAAGA
PF3D7_0422300	GCAGTAGGTGGAGGTACAGG	GAGGAGATGGCCACGAACAA

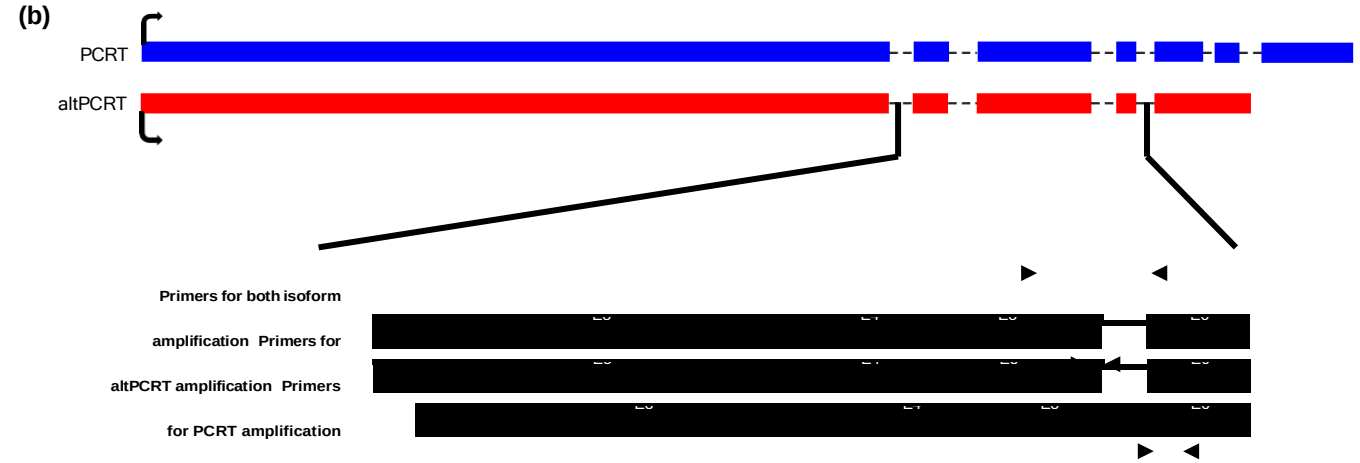

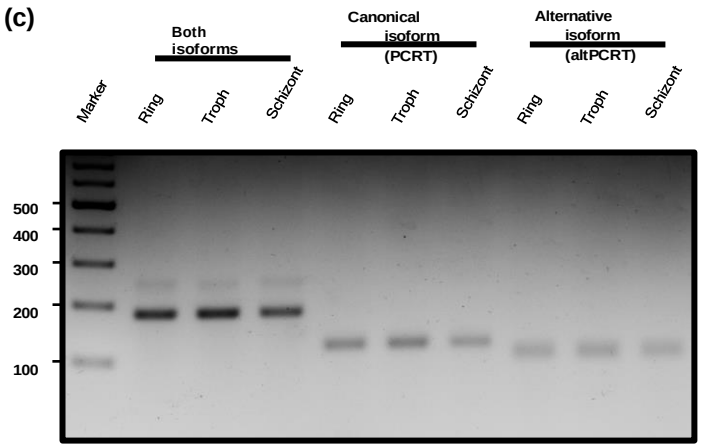

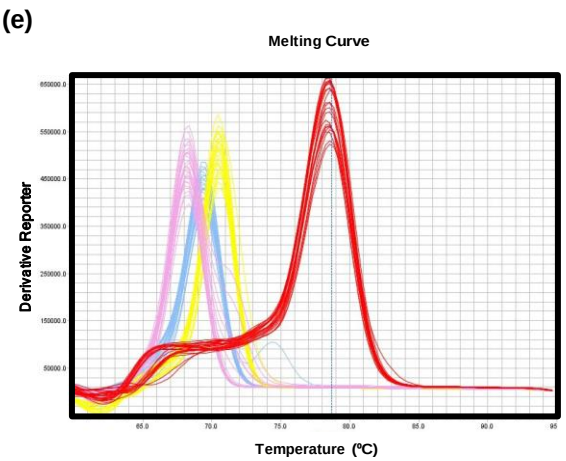

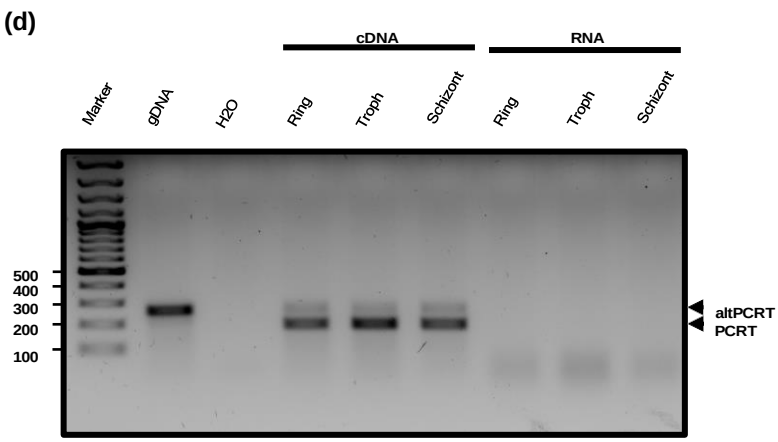

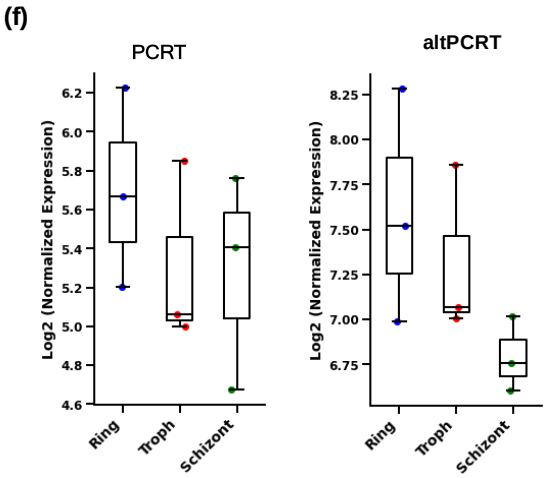

Figure S14: RT-PCR Confirmation of Canonical and Alternative Isoforms of *PF3D7_1138800.* (a) Primer sequences for amplification of both isoforms, each individual isoform as well as the reference gene (*PF3D7_0422300*) in conventional PCR and quantitative PCR. (b) Gene architecture of canonical isoform (*PF3D7_1138800.1*) and alternative isoform (*MSTRG.5058.9)*, along with amplified domains in respective isoforms for PCR. (c) Amplification by all pairs of primers was successful as shown by the isoform- specific PCR products at expected size for all the sample in the electrophoresis gel. (d) The absence of gDNA contamination was verified by incorporating reverse transcription-free samples. Negative controls comprised water, whereas genomic DNA (gDNA) served as the positive control. (e) Confirmation of isoform specificity of the products via quantitative PCR melting curve analysis.

(f) Isoform expression at different developmental stages of Plasmodium, as determined by qPCR employing the ddCt analysis method.

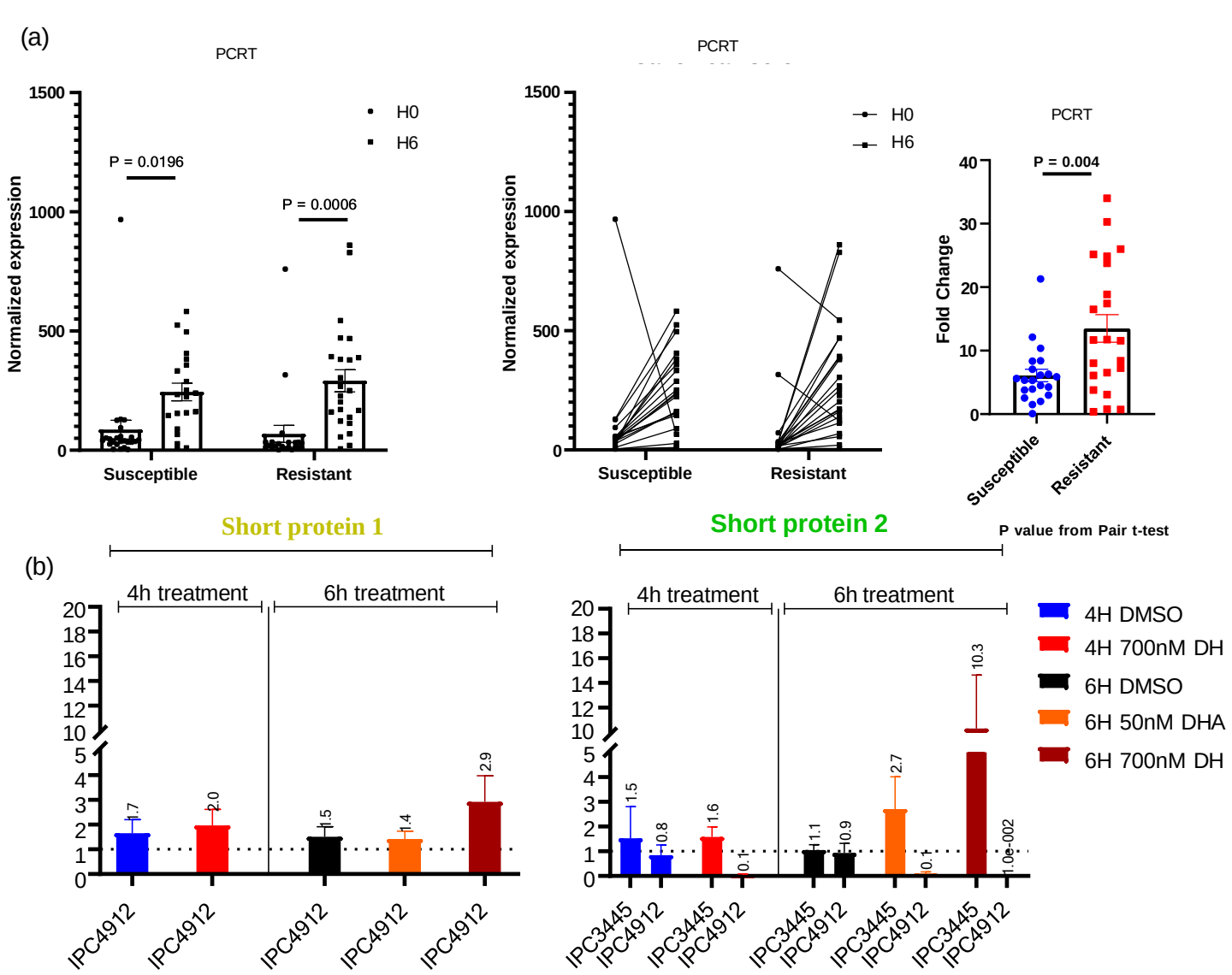

Figure S15: Expression profile of the PfWD11 from qPCR experiment. (a) Expression changes of the susceptible parasites and resistant parasites from 0 hours to 6 hours as groups (left) and as a pair (middle) respectively. Foldchange comparison between susceptible and resistant groups by Pairwise t- test. (b) The ratios of band intensities of Short isoform 1 and Short Isoform 2 relative to the full-length PfWD11 band intensity were measured with and without dihydroartemisinin (DHA) treatment in two resistant strains, IPC3445 and IPC4912. The duration of DHA treatments is indicated above the graph. The presence of Short isoform 1 appears to be much more pronounced in IPC4912 but only slightly induced in highest concentration of the drug after 6 hours treatment. Notably, the response to DHA shows opposite trends between the two strains for Short isoform 2: IPC3445 exhibited an increase in the levels of Short Isoform 2 relative to the full-length protein, while IPC4912 showed a decrease in these levels in a DHA concentration-dependent manner.

(a)

```
PCRT      1700 YHYNNTLVACGYYDNYVHLYDVRINSFIKRFKNNYPSNQGVTSLSFSKNG   1749
                ||||||||||||||||||||||||||||||||||||||||||||||||||
Non-PCRT  1701 YHYNNTLVACGYYDNYVHLYDVRINSFIKRFKNNYPSNQGVTSLSFSKNG   1750

PCRT      1750 RFLSYAGGYTNNLNLIDLAMDKFVEVEQKENMGININSFDELKYADNIRK   1799
                ||||||||||||||||||||||||||||||||||||||||||||||||||
Non-PCRT  1751 RFLSYAGGYTNNLNLIDLAMDKFVEVEQKENMGININSFDELKYADNIRK   1800

PCRT      1800 SIDGYLENDLMNIDERKNVSEIKKDDFSFYEDKILNIDFSYDNNLLVTAS   1849
                ||||||||||||||||||||||||||||||||||||||||||||||||||
Non-PCRT  1801 SIDGYLENDLMNIDERKNVSEIKKDDFSFYEDKILNIDFSYDNNLLVTAS   1850

PCRT      1850 CNNIIDFYNCSKASQEIKSTMDKKRIKLNNTKDKNRYVKLSKSFGVHYSN   1899
                ||||||||||||..::.
Non-PCRT  1851 CNNIIDFYNCSKGWEKN--------------------------------   1867

PCRT      1900 LISAKFTPENALLLFGINTLI   1920

Non-PCRT  1868 ---------------------   1867
```

(b)

Complete structure of PfWD11

PfKelch13 propeller-like domain at c-terminal of PfWD11

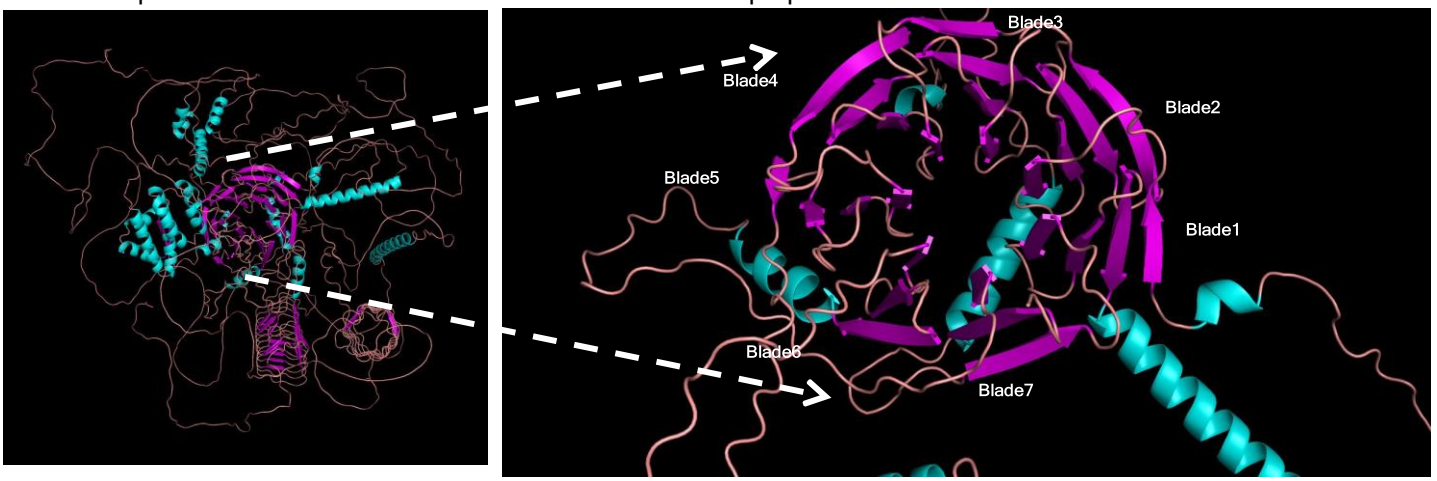

(c)

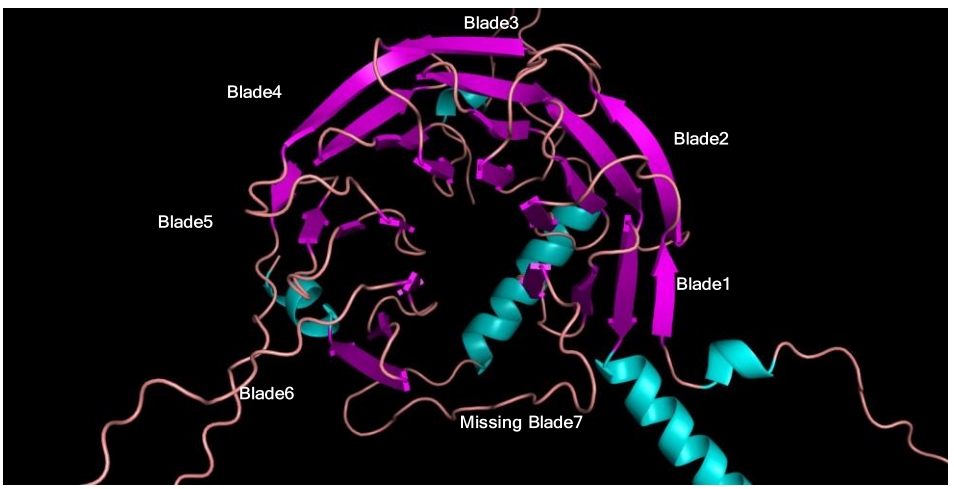

C-terminal of altPCRT of PfWD11

Figure S16: Putative effect of alternatively spliced PfWD11 on protein (a) Pair-wise sequence alignment of PCRT-altPCRT pair for PfWD11 protein. Retention of intron 5 in altPCRT leads to early truncation of the predicted open reading frame and indicates 58 missing amino acid residues compared to PfWD11 PCRT at the C-terminal. (b) Alpha fold predicted structure of PfWD11 was obtained from the Uniprot database and visualized in PyMol. Noticeably the c-terminal of the PfWD11 was found to have a propeller-like domain similar to PfKelch13 (whose propeller domain mutations are known resistance markers for Artemisinin

treatment). (c) The result of intron 5 retention leads to early truncation and missing blade 7, an integral part of the propeller domain, from the c-terminal structure of altPfWD11 predicted by Alphafold.

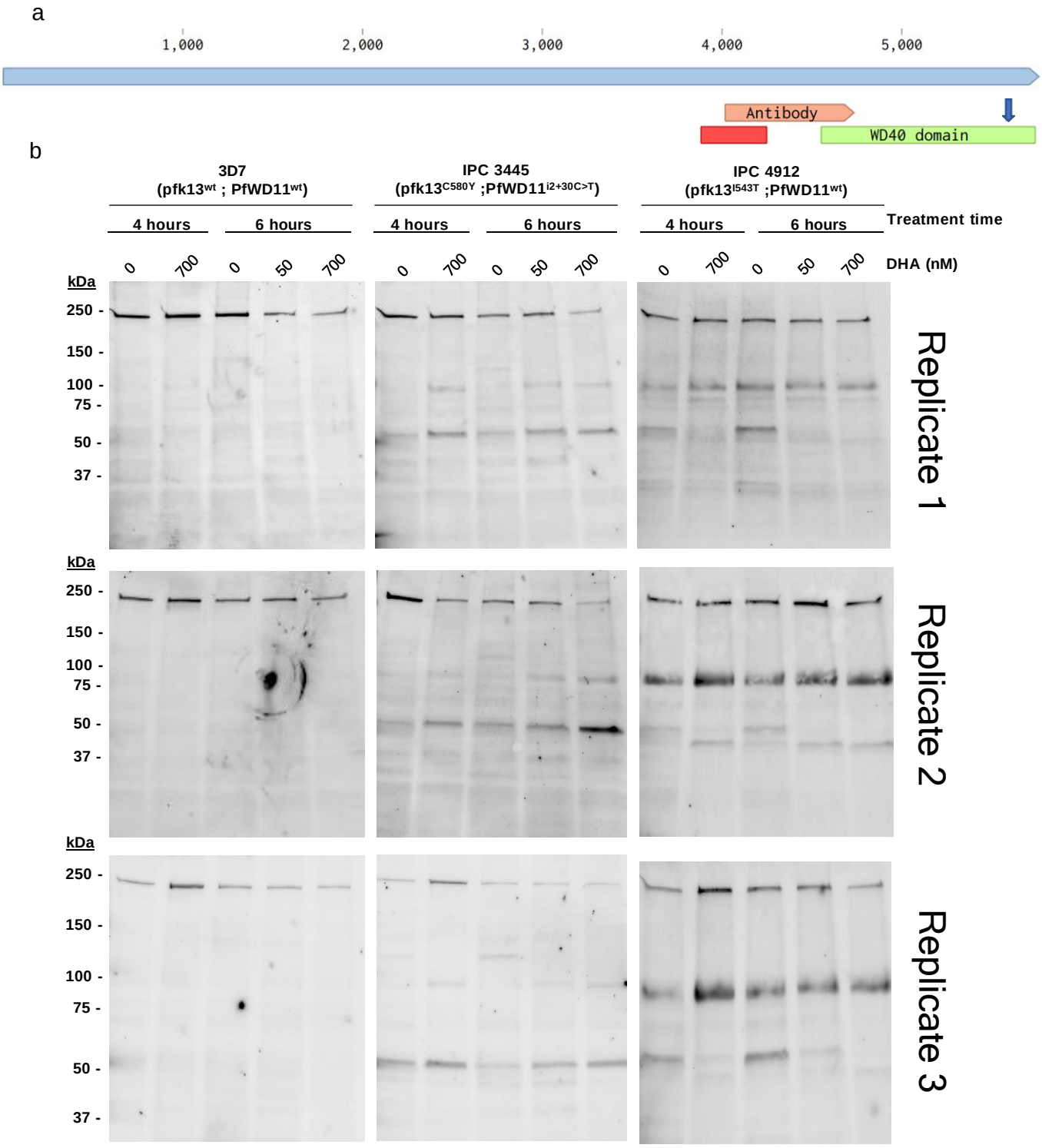

Figure S17: Full Images of PfWD11 Western Blots (a) Schematic diagram showing the epitope region used for generating the PfWD11 antibody.The antibody targets the region between N- terminal end of the predicted WD40 domain (green) and the C-terminal end of the predicted TAF5-like domain. An arrow indicates the potential protein truncation at the N-terminal end of the altPCT isoform retaining an intron (b)This figure shows complete western blot images from three biological replicates for the 3D7, IPC3445, and IPC4912 strains. Proteins were separated using 4-20% gradient polyacrylamide gels and the blots were probed with mouse anti-PfWD11 antibody followed by Alexa Fluor 647 anti-mouse secondary antibody. The 3D7 strain shows a single band at approximately 230- 250 kDa. In the resistant strains (IPC3445 and IPC4912), varying levels of PfWD11 processing are observed following DHA treatment.

(a)

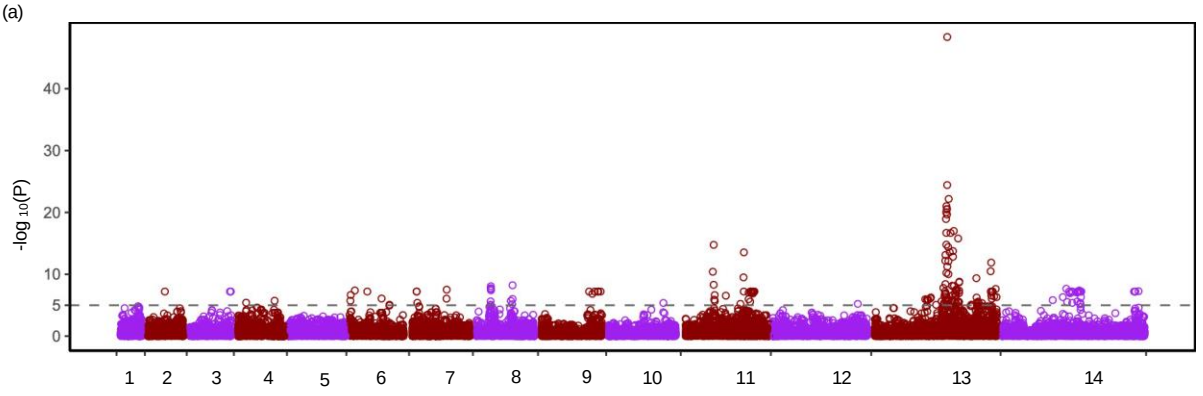

(b)

SNP ID	Annotation	Gene Name	Nucleotide change	Protein change	Euclidian distance	Pearson correlation
5:992428	intergenic_region	PF3D7_0523800-PF3D7_0523900	n.992428T>G	-	1.357	-0.291
5:1014838	intergenic_region	PF3D7_0524400-PF3D7_0524500	n.1014838T>C	-	0.512	0.878
6:98447	intron_variant	PF3D7_0602200	c.539+19A>G	-	0.452	0.909
6:552945	intergenic_region	PF3D7_0613500-PF3D7_0613600	n.552945T>C	-	0.424	0.967
6:637823	missense_variant	PF3D7_0615400	c.2352G>C	p.Met784Ile	1.307	-0.562
6:664920	missense_variant	PF3D7_0615900	c.2936G>C	p.Arg979Pro	0.411	0.934
6:684001	intergenic_region	PF3D7_0616400-PF3D7_0616500	n.684001T>C	-	0.364	0.950
6:708357	intergenic_region	PF3D7_0617000-PF3D7_0617100	n.708357A>G	-	0.693	0.949
6:806029	missense_variant	PF3D7_0619300	c.8524A>T	p.Ser2842Cys	0.449	0.980
6:825473	missense_variant	PF3D7_0619600	c.317G>T	p.Cys106Phe	1.744	-0.958
7:124510	missense_variant	PF3D7_0703200	c.2626G>A	p.Ala876Thr	0.414	0.970
7:126263	missense_variant	PF3D7_0703200	c.873G>T	p.Met291Ile	1.797	-0.973
7:182446	missense_variant	PF3D7_0704100	c.2411G>T	p.Gly804Val	0.262	0.980
7:187493	missense_variant	PF3D7_0704100	c.7458G>T	p.Lys2486Asn	0.287	0.980
7:211330	synonymous_variant	PF3D7_0704500	c.2172G>A	p.Pro724Pro	0.570	0.859
7:221722	synonymous_variant	PF3D7_0704600	c.7167C>T	p.Leu2389Leu	0.508	0.910
7:221815	synonymous_variant	PF3D7_0704600	c.7074G>T	p.Leu2358Leu	0.575	0.900
7:221825	missense_variant	PF3D7_0704600	c.7064A>C	p.Glu2355Ala	0.490	0.922
7:223299	missense_variant	PF3D7_0704600	c.5590G>A	p.Asp1864Asn	0.513	0.908
7:227124	missense_variant	PF3D7_0704600	c.1765A>T	p.Thr589Ser	0.561	0.896
7:227421	missense_variant	PF3D7_0704600	c.1468T>A	p.Cys490Ser	1.449	-0.740
7:229582	intergenic_region	PF3D7_0704600-PF3D7_0704700	n.229582G>A	-	0.708	0.739
7:450854	synonymous_variant	PF3D7_0710000	c.6465C>T	p.Tyr2155Tyr	0.559	0.933
8:405544	synonymous_variant	PF3D7_0808000	c.549T>C	p.Phe183Phe	0.378	0.937
8:405787	synonymous_variant	PF3D7_0808000	c.792T>C	p.Asn264Asn	0.323	0.951
8:857544	intergenic_region	PF3D7_0818800-PF3D7_0818900	n.857544T>A	-	0.437	0.923
8:858720	intergenic_region	PF3D7_0818800-PF3D7_0818900	n.858720T>A	-	NR/MA in Pf7k*	NR/MA in Pf7k*
8:1103478	intergenic_region	PF3D7_0825700-PF3D7_0825800	n.1103478A>T	-	1.742	-0.878
8:1103480	intergenic_region	PF3D7_0825700-PF3D7_0825800	n.1103480C>T	-	1.744	-0.878
8:1221692	missense_variant	PF3D7_0828300	c.992G>A	p.Ser331Asn	0.284	0.963
8:1233264	intergenic_region	PF3D7_0828600-PF3D7_0828700	n.1233264A>G	-	0.373	0.967
9:130213	intron_variant	PF3D7_0903100	c.554-21A>T	-	NR/MA in Pf7k*	NR/MA in Pf7k*
9:852446	intergenic_region	PF3D7_0920700-PF3D7_0920800	n.852446C>G	-	NR/MA in Pf7k*	NR/MA in Pf7k*
11:451811	intergenic_region	PF3D7_1111600-PF3D7_1111700	n.451811T>A	-	1.477	-0.793
11:710509	intron_variant	PF3D7_1118700	c.1080+79A>T	-	0.881	0.889
11:725049	missense_variant	PF3D7_1119300	c.691C>T	p.His231Tyr	0.239	0.979
11:744100	intergenic_region	PF3D7_1119600-PF3D7_1119700	n.744100A>T	-	0.357	0.958
11:754762	intergenic_region	PF3D7_1119900-PF3D7_1120000	n.754762C>T	-	0.318	0.954
11:756519	missense_variant	PF3D7_1120000	c.328A>C	p.Thr110Pro	NR/MA in Pf7k*	NR/MA in Pf7k*
11:767389	synonymous_variant	PF3D7_1120300	c.519A>G	p.Lys173Lys	0.393	0.936
11:770152	missense_variant	PF3D7_1120400	c.249G>A	p.Met83Ile	0.291	0.967
11:783289	missense_variant	PF3D7_1120600	c.167G>T	p.Arg56Ile	0.627	0.801
11:789263	intergenic_region	PF3D7_1120700-PF3D7_1120800	n.789263G>T	-	NR/MA in Pf7k*	NR/MA in Pf7k*
11:792550	synonymous_variant	PF3D7_1121000	c.354G>A	p.Gln118Gln	1.319	-0.219
11:902600	synonymous_variant	PF3D7_1123000	c.771T>C	p.Tyr257Tyr	0.293	0.972
11:904066	intergenic_region	PF3D7_1123000-PF3D7_1123100	n.904066C>A	-	1.745	-0.269
11:955213	synonymous_variant	PF3D7_1124100	c.1131C>T	p.Asn377Asn	0.879	0.887
11:1019514	missense_variant	PF3D7_1126100	c.2982T>G	p.Asn994Lys	1.077	0.879
11:1535276	intron_variant	PF3D7_1138800	c.4395+30T>C	-	0.437	0.964
12:2103598	missense_variant	PF3D7_1251600	c.482C>G	p.Thr161Arg	NR/MA in Pf7k*	NR/MA in Pf7k*
12:2107031	synonymous_variant	PF3D7_1251700	c.1026C>G	p.Val342Val	0.732	0.880
13:824979	missense_variant	PF3D7_1319900	c.1569G>T	p.Met523Ile	1.745	-0.269
13:926925	synonymous_variant	PF3D7_1322100	c.5955T>C	p.Asn1985Asn	NR/MA in Pf7k*	NR/MA in Pf7k*
13:1621165	intergenic_region	PF3D7_1340600-PF3D7_1340700	n.1621165T>A	-	0.506	0.961
13:1663525	missense_variant	PF3D7_1342200	c.206T>C	p.Leu69Ser	0.383	0.952
13:1675241	missense_variant	PF3D7_1342600	c.1159G>A	p.Gly387Ser	1.063	0.805
13:1677371	intergenic_region	PF3D7_1342600-PF3D7_1342700	n.1677371G>A	-	0.398	0.956
13:1678803	intergenic_region	PF3D7_1342700-PF3D7_1342800	n.1678803G>T	-	1.195	0.829
13:1696813	intergenic_region	PF3D7_1342900-PF3D7_1343000	n.1696813T>A	-	0.273	0.973
13:1700345	missense_variant	PF3D7_1343100	c.286A>G	p.Asn96Asp	1.055	0.484
13:1717359	missense_variant	PF3D7_1343400	c.2463T>G	p.Asn821Lys	0.233	0.975
13:1718288	missense_variant	PF3D7_1343400	c.3392A>T	p.Asn1131Ile	0.237	0.973
13:1739315	synonymous_variant	PF3D7_1343800	c.14172T>C	p.Asn4724Asn	0.701	0.951
13:1751770	missense_variant	PF3D7_1343800	c.1717C>T	p.Leu573Phe	0.748	0.968
13:1793121	missense_variant	PF3D7_1344700	c.1646T>C	p.Ile549Thr	0.795	0.954
13:1830612	intergenic_region	PF3D7_1345700-PF3D7_1345800	n.1830612A>G	-	0.599	0.927
13:1831070	intergenic_region	PF3D7_1345700-PF3D7_1345800	n.1831070A>T	-	0.646	0.915
13:1843088	intergenic_region	PF3D7_1346000-PF3D7_1346100	n.1843088T>G	-	NR/MA in Pf7k*	NR/MA in Pf7k*
13:1856973	missense_variant	PF3D7_1346400	c.4076G>A	p.Gly1359Asp	0.801	0.819
13:1908222	intergenic_region	PF3D7_1347600-PF3D7_1347700	n.1908222G>A	-	1.512	-0.610
13:1912767	missense_variant	PF3D7_1347800	c.706C>T	p.His236Tyr	0.299	0.958

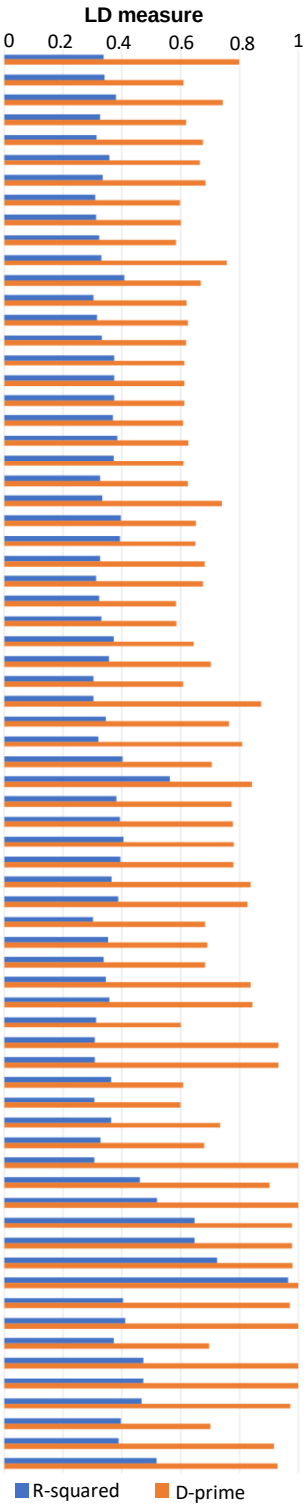

SNP ID	Annotation	Gene Name	Nucleotide change	Protein change	Euclidian distance	Pearson correlation
13:1912940	intergenic_region	PF3D7_1347800-PF3D7_1347900	n.1912940T>A	-	0.294	0.960
13:1913206	missense_variant	PF3D7_1347900	c.5440A>G	p.Thr1814Ala	0.302	0.958
13:1916603	missense_variant	PF3D7_1347900	c.2302A>G	p.Asn768Asp	0.311	0.955
13:1916698	missense_variant	PF3D7_1347900	c.2207A>G	p.Asn736Ser	0.328	0.952
13:1964252	missense_variant	PF3D7_1348800	c.4260C>A	p.His1420Gln	0.248	0.979
13:1987944	missense_variant	PF3D7_1349500	c.7671T>G	p.His2557Gln	1.451	-0.645
13:2004982	synonymous_variant	PF3D7_1350000	c.153A>G	p.Glu51Glu	0.506	0.935
13:2021209	intergenic_region	PF3D7_1350500-PF3D7_1350600	n.2021209T>A	-	0.448	0.888
13:2028330	synonymous_variant	PF3D7_1350900	c.309T>A	p.Leu103Leu	0.448	0.953
13:2700136	intergenic_region	PF3D7_1367700-PF3D7_1367800	n.2700136T>A	-	NR/MA in Pf7k*	NR/MA in Pf7k*
13:2824499	missense_variant	PF3D7_1371800	c.1126T>A	p.Phe376Ile	0.303	0.970
14:129153	missense_variant	PF3D7_1403400	c.1576G>C	p.Glu526Gln	0.328	0.966
14:325325	synonymous_variant	PF3D7_1408700	c.21144C>T	p.Ile7048Ile	0.235	0.993
14:862030	missense_variant	PF3D7_1420700	c.1860A>T	p.Gln620His	0.543	0.852
14:2081506	missense_variant	PF3D7_1450800	c.742G>C	p.Gly248Arg	0.960	0.849
14:2098642	synonymous_variant	PF3D7_1451200	c.213T>C	p.Asn71Asn	0.935	0.900
14:2310326	missense_variant	PF3D7_1456400	c.1903T>C	p.Ser635Pro	0.308	0.969
14:2367955	synonymous_variant	PF3D7_1457700	c.669G>A	p.Lys223Lys	0.381	0.953
14:2382247	synonymous_variant	PF3D7_1457900	c.6669G>A	p.Ser2223Ser	1.807	-0.967
14:2385550	synonymous_variant	PF3D7_1457900	c.9972C>T	p.Thr3324Thr	0.298	0.962

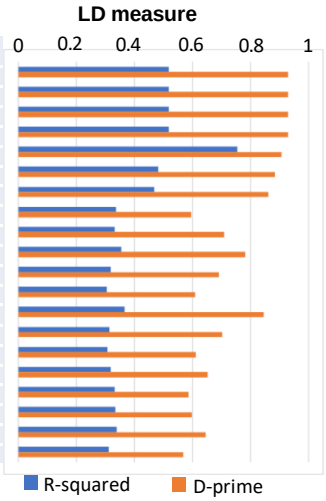

(c)

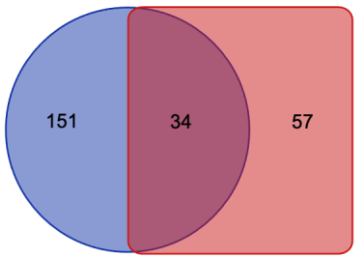

SNPs significantly associated with K13 C580Y as a phenotype

SNPs with high LD K13 C580Y

(d)

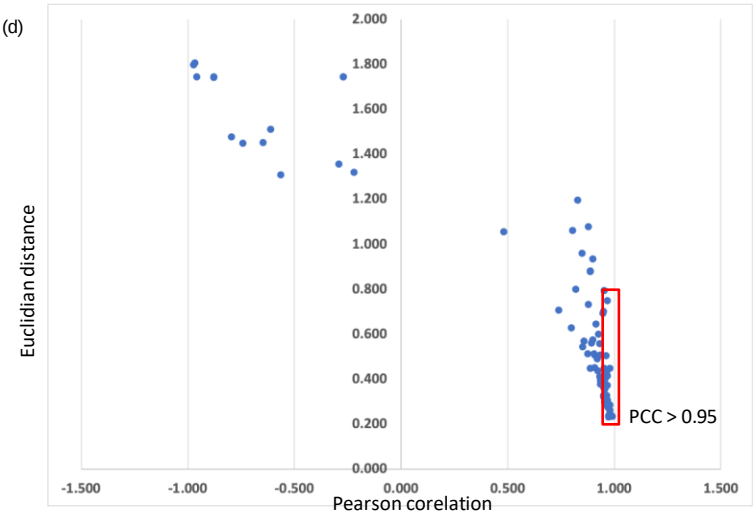

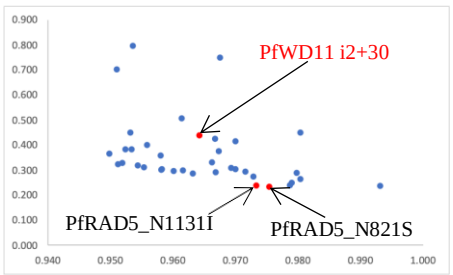

Figure S18: Temporal frequency changes of SNPs linked with K13 mutations (a) Manhattan plot of GWAS analysis considering K13 genotype as a binary phenotype. PfRAD5_N1131 (13:1718288) came out as the strongest marker in the absence of the K13 mutation, along with many others. PfWD11 i2+30 T>C did show significant association 1.05-E06. Complete results are provided as a supplementary table. (b) Upon inter-chromosomal linkage disequilibrium calculation was performed a total of 91 SNPs across the genome were found with high LD (R-squared >= 0.3 and d-prime > 0.5). Notably SNP PfRAD5_N1131 (13:1718288) was found high LD (=0.96) with K13C580Y. A moderate LD value between PfWD11 i2+30 and K13C580Y was found as 0.31. Additionally annotations of each SNP and how each of these SNPs' frequencies changed temporally compared to K13 C580Y mutation in three countries of eGMS (Thailand, Cambodia, and Vietnam) and presented as Euclidian distance and Pearson correlation. (c) Venn diagram showing SNPs significantly associated with K13 C580Y genotype (panel a) overlaps with SNPs with high LD with K13 C580Y genotype. (d) Euclidean distance and Pearson correlation were calculated for each SNPs with high LD with K13 C580Y and checked for similarity with K13 C580Y temporal changes. Scatterplot showing these two measures and highlighted PfRAD5 mutations (N1131I and N821S) and PfWD11 i2+30 mutation found as marker from GWAS analysis.